ORIGINAL ARTICLE

Infrared Thermography of the Pig Thorax: An Assessment of Selected Regions of Interest by Computed Tomographical and Anatomical Parameters

A. Menzel[1]*, C. Siewert[2], H. Gasse[3], H. Seifert[2], D. Hoeltig[1] and I. Hennig-Pauka[4]

Addresses of authors: [1] Clinic for Swine and Small Ruminants, Forensic Medicine and Ambulatory Services, University of Veterinary Medicine Hannover, Bischofsholer Damm 15, D-30173, Hannover, Germany;
[2] Institute for General Radiology and Medical Physics, University of Veterinary Medicine Hannover, Bischofsholer Damm 15, D-30173, Hannover, Germany;
[3] Institute of Anatomy, University of Veterinary Medicine Hannover, Bischofsholer Damm 15, D-30173, Hannover, Germany;
[4] Clinic for Swine, University of Veterinary Medicine Vienna, Veterinärplatz 1, 1210, Vienna, Austria

*Correspondence:
Tel.: +49 511 8567260;
fax: +49 511 8567684;
e-mail: anne.menzel@tiho-hannover.de

Summary

Current methods of diagnosis of respiratory diseases in swine are invasive, time-consuming and expensive. Infrared thermography (IRT) of the thorax might provide a new method of high specificity to select swine affected with lung alterations for further diagnostics. In this study, layer thickness of different tissues was determined in frozen thorax slices (FTS) by computed tomography (CT) and then related to skin temperatures measured by IRT in healthy pigs. The aim was to determine appropriate regions of interest (ROI) for evaluation of IRT images. Organ layer thicknesses measured in CT images correspond to those measured in FTS. Temperature differences between lung ROIs and abdomen ROIs were positively correlated with lung layer thickness at certain localizations, and negatively correlated with the thickness of the thorax wall and of inner organ layers. Reference values of differences between skin temperatures were established for two ROIs on the thorax with potential practical use for lung health status determination. Respective ROIs were located on vertical lines crossing the 7th (right) and the 10th (left) thoracic vertebrae. The presence of ribs affected skin temperature significantly.

Introduction

Porcine respiratory tract diseases are an large contributor to economic losses in the swine industry worldwide and are one of the main indications for antibiotic treatment in swine (Casal et al., 2007; Opriessnig et al., 2011). The current study undertakes clinical research aimed at the identification of pigs with inflammatory lung diseases which do not show clinical symptoms. It is hypothesized that an aetiological diagnosis is the correct basis for solving the herd problem.

Imaging procedures like computed tomography (CT) or digital radiography are of high sensitivity but are suitable for working practice. Neither CT nor radiography have been established as routine diagnostic methods in livestock medicine due to being time-consuming and both cost- and personnel-intensive (Brauer et al., 2011, 2012).

A more convenient imaging technique for the assessment of lung alterations is ultrasonography. The major disadvantage however is, that only lung alterations reaching the pleural surface can be found. Lung lesions covered by aerated lung tissue are undetectable (Heinritzi and Beisl, 1995; Reinhold et al., 2002; Hoeltig et al., 2008).

Infrared thermography as an imaging method for the detection of elevated body temperature, circulatory disorders or circumscribed organ inflammation. Such methodologies would be highly advantageous in swine medicine as its quick, inexpensive and non-invasive applicability.

The principle of IRT is the measurement of the temperature of the skin surface using a microbolometer

detector. Skin temperature is affected by continuous heat exchange between skin and environment, metabolic activity and blood circulation, as well as anatomical structures close to the body surface and skin characteristics (Zaproudina et al., 2008; Siewert et al., 2010a). In swine no reference values for skin temperature exist up to now, because no systematic study about temperature patterns of the body surface and its influencing factors have been performed.

In the following study, a systematic approach to evaluate IRT patterns of the pig thorax, with regard to anatomical aspects, was chosen to fill this gap of knowledge about skin temperature and its influencing factors under physiological conditions. Knowing the appropriate conditions and anatomical localization for measurement is the basis for the development of a non-invasive diagnostic method which will be applicable for a large number of animals on farms. For this reason, precise information about thickness and extend of organ layers in healthy pigs were collected from frozen cross-sections of the thorax and compared with the respective CT images. This was followed by a comparison with IRT images and the determination of regions of interest for temperature measurements. For the definition of health in this study, conventional diagnostic methods were extended and all relevant anatomical distances of the thorax were assessed. Patient-related parameters such as inner body temperature, breathing and heart rate as well as a standardized and optimized ambient temperature were taken into account during the establishment of reference values for IRT images of the porcine thorax.

Materials and Methods

Animals and housing
A total of 20 clinically healthy male castrated pigs (German Landrace), age ranging from 5 to 10 weeks and with a weight range between 9.2 and 17.4 kg were used in this study. All pigs were bred and raised in a closed breeding herd of high health status, routinely tested negative for *Actinobacillus pleuropneumoniae*, Porcine Reproductive and Respiratory Syndrome Virus (PRRSV), toxigenic *Pasteurella multocida,* endo- and ectoparasites. After arrival, all pigs used in this study were checked for antibodies against *Actinobacillus pleuropneumoniae* using an Apx-II-Enzyme-linked immunosorbant assay (ELISA) (Leiner et al., 1999). Animals were housed and cared under standardized conditions according to the Directive of the European Convention for the Protection of Vertebrae Animals Used for Experimental and Other Scientific Purposes (European Treaty Series, nos. 123 [http://conventions.coe.int/treaty/EN/treaties/html/123.htm] and

170 [http://conventions.coe.int/treaty/EN/treaties/html/170.htm]). All procedures were approved by the institutional review board as well as from the local ethics committee for animal experimentation (approval number: 33.14-42502-04-12/0835). Precautions aimed at avoiding unnecessary suffering were taken at all stages of the experiment. After arrival, an acclimatization period of at least 3 days started in which pigs adapted to the new environment and were monitored daily for clinical signs of illness. Systematically the following parameters were assessed daily: breathing noise, type of respiration, breathing rate, coughing, skin colour, posture, behaviour, feed intake, body temperature, and symptoms of gastrointestinal disorders as vomiting or diarrhoea. A clinical scoring system was applied to confirm that all twenty pigs that participated were clinically healthy, with scores ranging between 0.00 and 0.73 according to the classification by Hoeltig et al. (2009). Disease classification by clinical scores was: not affected (0–2.00), slightly affected (2.01–34.70), moderately affected (34.71–67.30) and severely affected (>67.30) (Hoeltig et al., 2009).

A commercial weaner pig diet (Deuka Primo, Deutsche Tiernahrung Cremer GmbH & Co. KG, Bremen, Germany) was given twice a day at certain points of time. On the examination days, no feed was given 15 h before induction of anaesthesia to the animals which were examined during that day to lower the risk of anaesthesia and the hypothetical effect of digestion onto surface temperature distribution.

Experimental setup
Pigs were divided into two groups with 10 pigs each. After clinical examination pigs were anaesthetized with 15 mg/kg body weight (bw) ketamine (Ursotamin®, Serumwerk-Bernburg AG, Bernburg, Germany) and 2 mg/kg bw azaperon (Stresnil®, Janssen-Cilag GmbH, Baar, Switzerland). IRT and CT were performed while patient-related parameters as body temperature, breathing frequency and cardiac frequency were recorded in parallel. The chest girth of the pigs was measured behind the elbow using a tape measure. After examination procedures, all pigs were euthanized with 60 mg/kg bw pentobarbital (Euthadorm®, CP-Pharma, Burgdorf, Germany).

Pigs out of group 1 served for the production of frozen thorax slices (FTS), while pigs from group 2 were necropsied, and lung tissue was sampled for histological and microbiological examination.

Computed tomography
A third generation single-slice CT scanner (Philips Tomoscan M, Philips Medical Systems, Germany) using defined

settings for scanogram and volume scan (tube voltage 120 kV, current 40 mA, slice thickness 7 mm, reconstruction interval 5 mm, pitch 1.5) was used for computed tomographical examination of the thorax. Anaesthetized pigs were positioned headfirst in sternal recumbency and were scanned from the cranial thoracic aperture to the caudal end of the lung. Conventional window settings for visual analysis of CT images of lung tissue were used (window width: 1500 Hounsfield Units (HU), window level: -600 HU). To save and evaluate absorption and density measurements of the CT scans, a standard Windows PC and an image analysis software package (eFilm, eFilm Medical Inc., Toronto, Ontario, Canada) were used.

All images were assessed from cranial to caudal by the same investigator. A scoring system was used to quantify lung tissue alterations (Brauer et al., 2011). Each transverse cross-section was divided into four quadrants (left dorsal, right dorsal, left ventral, right ventral) by axial and horizontal boundary lines. Horizontal lines were tangential to the ventral edge of the bronchus trachealis, or tangential to the lung bifurcation in the precardial and cardial sections, and tangential to the oesophagus in the postcardial sections. Axial boundary lines were crossing the vertebral body and were placed right-angled to the horizontal lines. All transverse cross-sections were scanned for pneumonic changes as consolidations and ground glass opacities. If at least one consolidation or ground glass opacity was detected within one quadrant, one scoring point was counted, so that a maximum score of four could be reached for one transversal CT image. In addition, tissue densities were measured within a circular region of interest (ROI) with an area of 120 mm^2 in the centre of a consolidation. ROIs did not contain air ways, blood vessels or other interfering elements. The mean density (mean HU) was translated from the optical speckles in the selected area by the imaging analysis software. Within each transversal cross-section only the consolidation with the highest density was scored as follows: $<$ (-550) HU no scoring points; from (-550) to (-150) HU two scoring points; $>(-150)$ HU four scoring points. Based on these two scorings, the maximal total score for each single transverse cross-section was eight. The mean score of all transverse cross-sections was the final CT score per pig (maximal reachable score of eight).

Anatomical examination

After clinical examination, pigs were anaesthetized and CT and IRT imaging were performed. Immediately after imaging procedures pigs were euthanized and either necropsied ($n = 10$) or frozen ($n = 10$). To evaluate the accuracy of tissue thickness measurement in the CT images, frozen thorax slices (FTS) of the same pigs ($n = 10$) were

cut and measured. To guarantee the same position during both imaging procedures and slicing, the pigs were fixated in deep anaesthesia onto a plastic plank in sternal recumbency with front legs stretched and strapped forward and the hind limbs extended and strapped backwards.

The pigs were euthanized (80 mg pentobarbital/kg bw intravenously), and intubated subsequently. Then, the lung was inflated with air before the endotracheal tube was blocked with a clamp to prevent air leakage. Inflated air volume approximated the tidal volume of the animals about 10 ml air volume per kilogram bodyweight (Stahl, 1967; Klein, 1999). Inter-vertebral spaces of the thoracic region between thoracic vertebrae (TV) were marked for later construction of reference lines for cutting. The bodies were placed in a deep freezer at $-20°C$ for at least 48 h. Frozen bodies were cut into slices at the marked positions using an electrical chain saw. Head and caudal part of the body beyond the last ribs were discarded. Slices containing lung tissue or ribs were marked on the cranial surface, labelled and kept frozen.

Slices were divided into four quadrants according to the respective CT transverse cross-sections (Fig. 1). The diameter of the thorax was determined by the vertical line
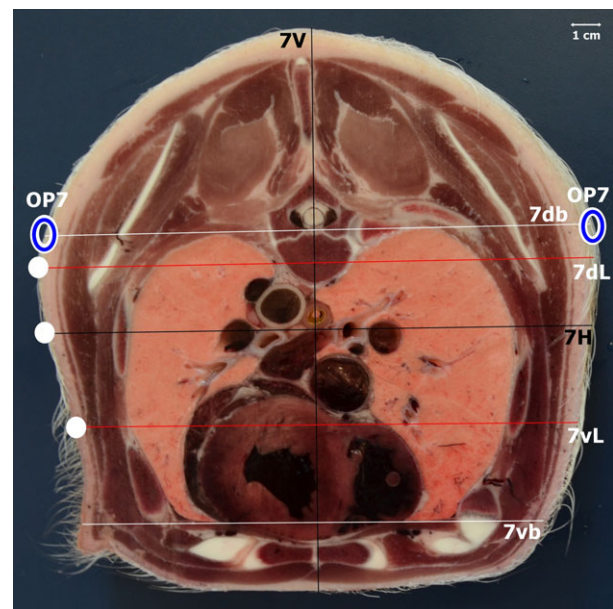

Fig. 1. Frozen thorax slice, caudal view, transverse section at the 7th thoracic vertebra, db = dorsal lung border, vb = ventral lung border, blue ring = anatomical orientation point on the level of the 7th thoracic vertebras (OP7) on the left and right side of the thorax, white dots = position of the centres of the regions of interest (ROI) for IRT image evaluation, 7Hl-7Hr = horizontal line dividing the ventral from the dorsal part of the thorax positioned at the ventral wall of the oesophagus. Auxiliary lines between the upper and middle thirds of the dorsal part (7dLl-7dLr) and between the two halves of the ventral part (7vLl-7vLr) of the lung.

between the respective vertebral body and the sternum (x.TV, x = 5th, 7th or 10th thoracic vertebrae). A horizontal line (H) dividing the ventral part from the dorsal part of the thorax was positioned at the ventral tracheal wall, at the lung bifurcation, or at the oesophagus. Horizontal lines, tangential to the lung boundaries in the dorsal (dorsal border = db) and ventral (ventral border = vb) halves of the thorax were placed parallel to H. Distances between db, vb, and H were measured and subdivided into three dorsal and two ventral segments, to create two additional auxiliary lines: between the upper and middle thirds of the dorsal area (dL) and between the two halves of the ventral area of the lung (vL). Thickness of skin, muscle, lung tissue, airways, liver and heart tissue was measured along the three auxiliary lines (db, H, vb) on both sides, i.e. left and right. Line x.TV divided each line into a left and a right part (dLl and dLr, Hl and Hr, vLl and vLr).

For comparison of FTS with the respective CT images, lines dL, H, and vL were positioned in the CT images in the same way (Fig. 2).

The thickness of different tissue layers was measured along the auxiliary lines on the left and the right side of the body. The thickness of a superficial layer (SL) presenting skin, fat tissue, muscles and ribs, of an intermediate layer representing the lung (IL), and airways and of a deep layer (DL) presenting vertebrae, inner muscles, heart and liver were calculated and encoded for statistical evaluation. Within each slice, 18 distances were determined (SL, IL, DL along three auxiliary lines at the right and left body side). Measured distances within FTS and CT images were compared subsequently.

Infrared thermographical examination

The infrared thermographical examination was the main subject of this study. The aim was to assess the influence of layer thickness of different tissues onto the surface temperature of the thorax.

In anaesthetized pigs metal markers were fixed at the 5th, 7th, 10th and 13th rib left and right beside the spine. Afterwards pigs acclimated in a cooling chamber with an average ambient temperature of 13.2°C for 30 min. Prior to and after this acclimatisation period heart frequency, respiratory rate and body temperature were recorded and IRT images were made from the left and right side of the body after the cooling period. The IRT-camera (VarioCAM hr Inspec, Infratec, Dresden, Germany) was fixed in a constant distance right-angled to the thorax. Presetting of the camera was a premium mode with a camera-internal repeated calibration prior to IRT imaging (Infratec, 2009). Thus, a continuous balancing of inhomogeneities in the microbolometer array was possible. An emissivity of 0.96, which is a good assumption for skin with little hair, was preset (Schuster and Kolobrodov, 2004; Diakides and Bronzino, 2008). Picture matrix was 384×288 pixels and the thermal resolution was 50 mK. Additionally, a reference body with constant room temperature placed next to the pig was recorded on each image as an internal standard (Fig. 3).

Environmental parameters such as room temperature, relative humidity and air movement were recorded using an indicating instrument (Testo 400, Testo AG, Lenzkirch, Germany).
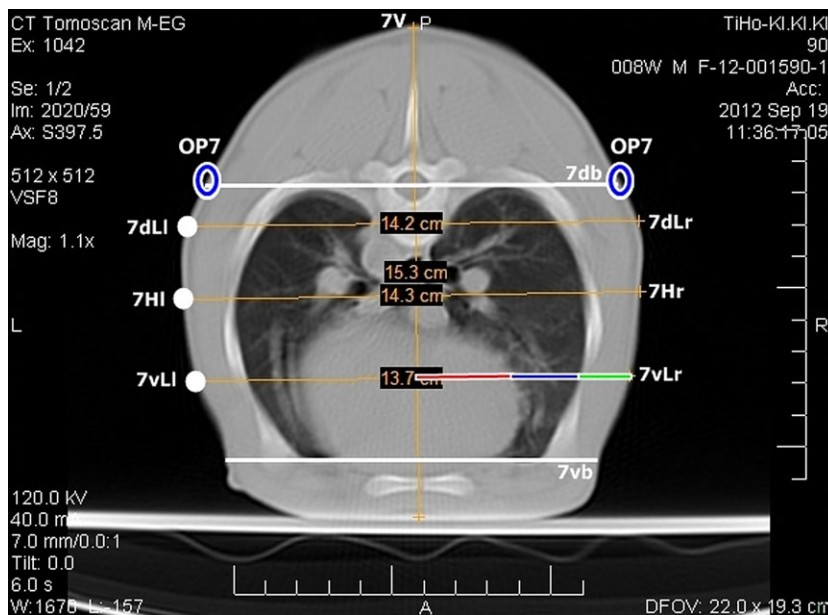

Fig. 2. CT image, Thorax, caudal view, transverse section at the 7th thoracic vertebra, blue rings = anatomical orientation point on the level of the 7th thoracic vertebras (OP7) on the left and right side of the thorax, white dots = position of the centres of the regions of interest (ROI) for IRT image evaluation, 7Hl-7Hr = horizontal line dividing the ventral from the dorsal part of the thorax positioned at the ventral wall of the oesophagus. Auxiliary lines between the upper and middle thirds of the dorsal part (7dLl-7dLr) and between the two halves of the ventral part (7vLl-7vLr) of the lung. Red line = deep layer (DL), blue line = intermediate layer (IL), green line = superficial layer (SL), numbers in black boxes = total length of the three horizontal orange lines (7dLl-7dLr, 7Hl-7Hr and 7vLl-7vLr) and the vertical line 7V.
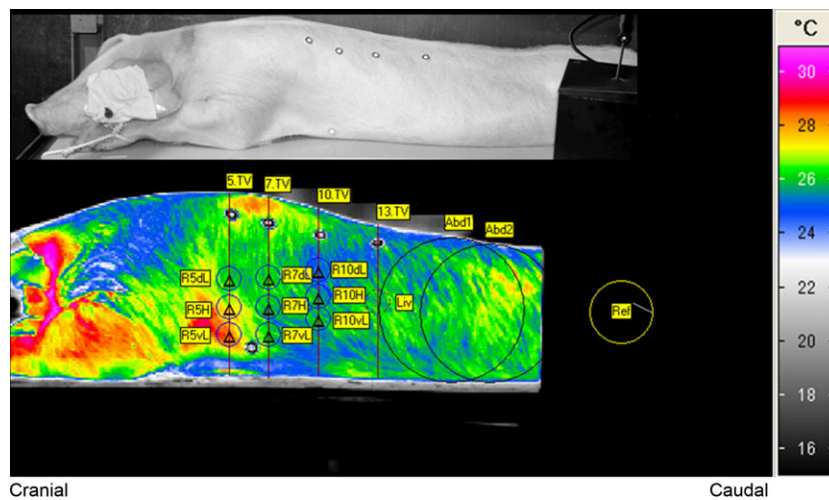
Fig. 3. IRT image of pig in sternal recumbency with ROIs and reference lines, left view, TA = 10.2°C, colour range: SW-VarioCam, temperature range = 15–31°C, picture matrix: 384 × 288 pixel, emissivity of 0.96. 5.TV = vertical line of the 5th thoracic vertebra (TV), 7.TV = vertical line of the 7.TV (this line served as reference line to adapt the scale of the CT to the IRT images), 10.TV = vertical line of the 10.TV, 13.TV = vertical line of the 13.TV, Ref = ROI of the reference body, Abd1 and Abd2 = abdominal ROIs, R5 dL = ROI of line dL of the 5th thoracic vertebra (TV), R5H = ROI of line H of the 5.TV, R5vL = ROI of line vL of the 5.TV, R7 dL = ROI of line dL of the 7.TV, R7H = ROI of line H of the 7. TV, R7vL = ROI of line vL of the 7.TV, R10 dL = ROI of line dL of the 10.TV, R10H = ROI of line H of the 10. TV, R10vL = ROI of line vL of the 10.TV.

For analysis of IRT images a standard Windows PC and an image analysis software package (Irbis3, InfraTec GmbH, Dresden, Germany) were used.

The metal markers served as anatomical landmarks (Orientation points = OP) to find the exact positions of the lines xdL, xH and xvL (x = 5th, 7th or 10th thoracic vertebra) in the IRT images which correspond to the auxiliary lines in the FTS and CT images.

To transfer the positions of xdL, xH and xvL and their information about the surface temperature to the anatomical conditions, the scale of the CT image was adapted to the scale of the IRT image. Line 7.TV in the CT image was transferred to the IRT image in the ratio 2:1 crossing OP7 perpendicular to the ventral bodyline of the pig (Fig. 3). This facilitates the correct position of ROIs onto the IRT image. The other lines 5.TV, 10.TV and 13.TV were positioned parallel to 7.TV and crossed their corresponding OPs in the IRT image. Onto each of the lines 5.TV, 7.TV and 10.TV, three ROIs (R) for the lung area (RxdL, RxH, RxvL) were located. To make sure that the centre points of these ROIs had exactly the same position as the lines xdL, xH and xvL in the CT images, the distances between the three auxiliary lines and the dorsal bodyline were measured in the CT images and were also transferred in the ratio 2:1 to the IRT images. Each of the nine positions was marked as the centre of the corresponding ROI with a diameter of 1 cm (Fig. 3). In addition, two ROIs were positioned in the abdomen in order to cover as much as possible of the abdominal area (Abd$_1$, Abd$_2$). Abd$_1$ touched tangentially the dorsal and ventral bodyline as well as OP13. Abd$_2$ was positioned behind Abd$_1$ tangentially to dorsal and ventral bodyline and covered the remaining part of the abdomen. Maximal temperature (ϑ_{Max}) and standard deviation were documented. Another ROI (Liv) with a diameter of 1 cm was located on line 13.TV to provide information about the surface temperature influenced by underlying liver tissue. The last ROI (Ref) with a diameter of 2.5 cm presented the reference body temperature.

To overcome measurement inaccuracy of absolute temperatures depending on the time interval between switching on the camera and the measurement as a time-dependent drift error, temperature differences between ROIs at two defined body localizations were determined as an allocation base. Surface temperature differences were calculated between average temperatures of lung ROIs and the maximal temperatures out of Abd$_1$ or Abd$_2$ according to the equation (1):

$$\Delta\vartheta\,Rx = \vartheta_{maxAbd1,Abd2} - \vartheta_{meanRx} \qquad (1)$$

Histological examination

To confirm the lung health status, lung tissue was taken after necropsy of 10 pigs for histological and microbiological examination. Three lung localizations were sampled: dorsal surface of the lung in the area of the lobus caudalis pulmonis dexter/sinister and lobus cranialis pulmonis

dexter (left and right diaphragmatic lobes and right apical lobe of lung). Each sample was divided into three parts. Part 1, for histological examination, was fixed in 10% formalin containing 2% calcium acetate. Histological sections were stained with haematoxylin-eosin (HE, haemalaun after Delafield). For viral examination, part 2 was immediately processed for multiplex Polymerase Chain Reaction (PCR) according to the protocol of Harder and Huebert (2004) for detection of *Mycoplasma hyorhinis*, *Mycoplasma hyopneumoniae*, Porcine Reproductive and Respiratory Syndrome Virus EU and US type, Influenza A virus, Porcine Circovirus 2, Porcine Cytomegalie Virus and Porcine Respiratory Coronavirus in the Institute of Virology, University of Veterinary Medicine, Hannover. In parallel, part 3 was provided for bacteriological examination of colonizing bacterial species according to routine protocols in the Institute of Microbiology, University of Veterinary Medicine, Hannover. Briefly, lung tissue was plated on conventional culture plates and inoculated over night at 37°C, followed by subculturing of single bacterial colonies and further characterization of bacterial species.

Statistical analysis

SAS® statistical software (SAS Institute Inc., Cary, NC, USA) was used for data analysis. Because parameters were not normally distributed, correlations between parameters were assessed by calculating the Spearman's Correlation coefficients with *P*-values <0.05 considered significant. Differences in tissue layer dimensions measured by CT and FTS were evaluated using the Wilcoxon's signed rank test. Comparison of pigs with and without rib presence below the ROIs was performed using the Wilcoxon's two-sample test.

Results

Respiratory health status of the pigs

The good respiratory health status of the pigs was confirmed by several examination techniques. Health parameters are summarized in Table 1. By clinical and CT scores all animals were assessed as healthy. No gross pathological lung alterations were found during necropsy. Histological examination of all lung tissue samples resulted in a mild interstitial pneumonia.

None of the respiratory pathogens were detected by PCR. By bacteriological examination commensals and environmental bacteria were isolated from lung tissue: non-haemolytic Staphylococci, coagulase-*negative Staphylococci*, *Staphylococcus aureus*, *Staphylococcus hyicus*, *Bacillus* spp., *E. coli*, gram-negative NAD-related bacteria,

Table 1. Health parameters of the examined pigs (*n* = 20)

	Clinical Score Reference range for healthy pigs 0–2.0 (Hoeltig et al., 2009)	CT score (HU) Reference range for healthy pigs 0–1.7 (Brauer et al. 2012)	Inter-mediate layer thickness 7vLlLr [mm]	Inter-mediate layer thickness 10vLlLl [mm]	Mean absolute surface temp. R7vLr [°C]	Mean absolute surface temp. R10vLl [°C]	Maximal absolute surface temp. right Abd₁, Abd₂ [°C]	Maximal absolute surface temp. left Abd₁, Abd₂ [°C]	IRT Δ𝜗 R7vLr [°C] (Δ𝜗 R7vLr = 𝜗maxAbd1, Abd2 - 𝜗meanR7vLr)	IRT Δ𝜗 R10vLl [°C] (Δ𝜗 R10vLl = 𝜗maxAbd1, Abd2 - 𝜗meanR10vLl)
Median	0.1	0.32	21	7	26.4	26.31	28.84	29.23	2.67	2.40
Range	0.01–0.73	0.08–1.50	11–31	3–15	23.97–28.79	24.67–28.14	26.52–30.46	26.62–31.41	0.02–6.60	(−0.26)–4.50

Haemophilus parasuis, *Klebsiella* spp., *Proteus* spp., *Pseudomonas* spp., *Aeromonas* spp., non-haemolytic Streptococci, beta-haemolytic Streptococci, *Rhodococcus equi*.

Reproducibility of anatomical measurements in frozen thorax slices and CT images

In summary, age was not correlated with horizontal distances, while weight and chest girth were always positively correlated with the distances xV and xH ($P < 0.05$).

Three FTSs at the level of 5.TV, 7.TV and 10.TV and respective CT images were dimensioned in each individual pig ($n = 10$), including 25 measurements for each TV, so that in total 75 distances were compared between the both techniques using the Wilcoxon signed rank test. Approximately half of the measured distances (46.7%) were significantly different from each other, but with a very small mean difference of 1.3 mm with standard deviation of 4.5 mm. A tendency towards a positive deviation for the FTS was found. The maximal difference was 13.6 mm. The overall mean value of all distance measurements in FTS and CT images were highly concordant. In FTS and CT, the lung was found to extend up to the 13th TV on both sides during maximal inspiration. Descriptive statistical parameters for the distances of the three tissue layers (left and right summarized from all slides) are shown in Table 2. Means and standard deviations recorded for FTS and CT images were similar.

Correlation of skin temperature difference with underlying tissue layer thickness

Temperature measurements at specific ROI positions resulted in significant correlations of temperature differences with tissue layer distances (Table 3).

Most interesting were positive correlations of temperature difference with the extent of the intermediate layer containing the lung at the ventral part of the thorax in the level of the 7.TV on the right side (7vLILr: Spearman rank correlation coefficient (r_s) = 0.47, $P = 0.038$) and 10. TV on the left side (10vLILl: $r_s = 0.50$, $P = 0.024$) as well as negative correlations with the extent of superficial layer (dorsal and medial part of the thorax at the level of the 7.TV (7dLSLr: $r_s = -0.64$, $P = 0.002$, 7HSLr: $r_s = -0.59$, $P = 0.006$)) and the deep layer (ventral part of the thorax at the level of the 10.TV (10vLDLr: $r_s = -0.56$, $P = 0.011$)).

Because of surface temperature difference being influenced by lung layer thickness at above mentioned localizations, R7vLr and R10vLl were selected as reference ROIs for the establishment of reference ranges of temperature difference according to the equations (2) and (3):

$$\Delta\vartheta\, R7vLr = \vartheta_{maxAbd1,Abd2} - \vartheta_{meanR7vLr} \quad (2)$$

and

$$\Delta\vartheta\, R10vL1 = \vartheta_{maxAbd1,Abd2} - \vartheta_{meanR10vL1} \quad (3)$$

Data of both parameters were not normally distributed, so that the ranges of minimal and maximal temperature differences at both localizations were depicted as preliminary reference ranges (Table 1).

Internal body temperatures descended during anaesthesia and within the cooling chamber. Prior to anaesthesia at room temperature internal body temperatures were within the range of 38.6–39.2°C, while during anaesthesia and 30 min in the cooling chamber temperatures were within the range of 32.0–35.9°C. Inner body temperatures were positively correlated with absolute surface temperatures of both ROIs R7vLr ($r_s = 0.63$, $P = 0.003$) and R10vLl ($r_s = 0.66$, $P = 0.002$) measured during anaesthesia.

Table 2. Descriptive statistical parameters for measured distances in FTS and CT images. Measurements of superficial layer (SL), intermediate layer containing the lung (IL) and deep layer (DL) from all slices were summarized

	SL CT [mm]	SL FTS [mm]	IL CT [mm]	IL FTS [mm]	DL CT [mm]	DL FTS [mm]
Mean	19.4	22.1	30.7	31.3	18.7	19.0
Range	12.1– 36.1	14.3–44	1.7–51.8	5.3–59.4	0–61	0–63.1
Median	17.1	19	36.4	34.6	10.8	12.2

Table 3. Correlation of tissue lung layer thicknesses with temperature differences (r_s = Spearman's rank correlation coefficient and *P*-values)

	$\Delta\vartheta_{7vLILr}$	$\Delta\vartheta_{10vLILl}$	$\Delta\vartheta_{7dLSLr}$	$\Delta\vartheta_{7HSLr}$	$\Delta\vartheta_{10vLDLr}$
Intermediate layer thickness (containing lung)	$r_s = 0.47$ $P = 0.038$	$r_s = 0.50$ $P = 0.024$	$r_s = 0.16$ $P = 0.508$	$r_s = -0.24$ $P = 0.307$	$r_s = -0.18$ $P = 0.438$
Superficial layer thickness (containing muscle, ribs and skin)	$r_s = -0.11$ $P = 0.660$	$r_s = 0.1$ $P = 0.68$	$r_s = -0.64$ $P = 0.002$	$r_s = -0.59$ $P = 0.006$	$r_s = 0.25$ $P = 0.291$
Deep layer thickness (containing heart, liver, inner muscles or vertebrae)	$r_s = -0.39$ $P = 0.088$	$r_s = 0.29$ $P = 0.218$	$r_s = 0.27$ $P = 0.247$	None present deep layer	$r_s = -0.56$ $P = 0.011$

Influence of presence of ribs on skin temperature

All ribs examined in the FTS contained active bone marrow. Ribs were present in underlying tissue of nearly all ROIs in most pigs. Approximately 20% of pigs showed no ribs in underlying tissue of ROIs on the left side at the level of 5th vertebra at the ventral part of the thorax (5vLl). For further evaluation, pigs were divided into a group with a rib (group A, $n = 15$) and a group without a rib (group B, $n = 5$) at that position. The difference in temperature difference between both groups was significant (Wilcoxon two sample test, $P = 0.011$, Fig. 4).

Discussion

The aim of this study was to evaluate the influence of different tissue layer thicknesses onto the surface temperature of the porcine thorax. As a basis for future development of IRT in pigs for the diagnostic of respiratory diseases, most appropriate ROIs for temperature measurements were determined. In future studies, a successful detection of gross pathological lung lesions in pigs by IRT under suitable ambient temperature conditions might be possible (Siewert et al., 2010b).

In general, infrared imaging is a simple and quick method for the measurement of the surface temperature distribution. Measurement results of IR cameras with uncooled microbolometer chips are generally influenced a) by the surrounding temperature, b) by the time interval between power-on and measurement as well as by, c) a time-dependent drift error (Hartmann and Fischer, 2001). For this reason difference temperatures were measured between two ROIs on the body surface as a practical approach to overcome these technical device errors. A precondition to measure temperature differences between different ROIs is the specification of two anatomical localizations which can be repeatedly found in the IRT image. At these anatomical localizations ROIs can be positioned. Difference imaging eliminates off-set errors which vary between different IRT images. In the used IR camera the absolute measuring accuracy was ±1.5°C according to the manufacturer's instructions.

In this study, the high respiratory health status of pigs was important to establish preliminary reference values for difference thorax temperatures in healthy pigs. Respiratory health was confirmed by different examination methods, because a clinical examination alone is insufficient to draw conclusions about gross pathological changes (Straw et al., 1990; Brauer et al., 2012).

For detection of respiratory disease in living pigs CT examination can serve as a diagnostic gold standard (Brauer et al., 2012).

In euthanized pigs the assessment of gross pathological changes in combination with histological findings can be regarded as a gold standard. In contrast with that, the interpretation of detected microorganisms is often difficult, as not only commensals and environmental bacteria but also pathogenic microorganisms can be detected regularly also in healthy pigs. Therefore, the isolation of microorganisms by itself has no significance for the health status of pigs (Hensel et al., 1994). In the examined pigs, no pathogens were detectable and no gross pathological changes were found. Lung tissue histology resulted in a mild interstitial pneumonia which is regularly found in healthy pigs and might be a balanced reaction to commensal bacteria or abiotic factors (Hennig-Pauka et al., 2012). Hansen et al. (2010) found interstitial lung lesions in 50% of the control pigs previously defined as healthy and at least one pathogen was detected from lung samples. In an extensive study for the assessment of lung health status of fattening pigs, which were held in different housing systems, an increase of lymphocytes and histiocytes within the inter-alveolar walls was also detected in all healthy pigs, which is consistent with the diagnosis of interstitial pneumonia in the study (Rieger, 2005).

The used CT equipment was not appropriate to detect these interstitial tissue alterations, due to slices as narrow as 1 mm and a longer examination time being necessary (Brauer et al., 2012). CT Scores reflected mild lung tissue changes in several pigs. They may be attributed to the
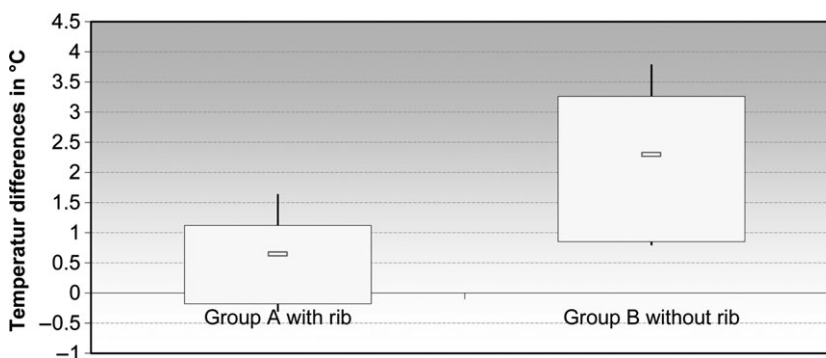

Fig. 4. Influence of presence of ribs on temperature differences at location 5vL left. Box-plot showing the ranges of temperature differences between the lung ROI temperature at the left ventral thorax side at the level of the 5th vertebra (5vLl) and the maximal abdominal temperature. In group A ($n = 15$) pigs had ribs at that lung ROI location, while in group B ($n = 5$) pigs had no ribs at that location.

fact, that imaging was not always performed at maximum inspiration, which is impossible in living, anaesthetized pigs (Myer, 1979; Silverman and Suter, 1975). Another reason for false positive findings in CT images might be attributed to fluid accumulation in the ventral parts of the lung due to ventral recumbency. In this posture lung tissue is gravitationally compressed during the respiratory cycles, as the pig was not in its natural standing position (Wandtke et al., 1986; Verschakelen et al., 1993). To minimize fluid accumulation pigs should be as short as possible in anaesthesia prior to CT examination.

Anatomical measurements of tissue layer thickness by CT as well as in frozen thorax slices differed only a few millimetres, so that no relevant practical impact existed. Because CT images were highly corresponding to the natural anatomy of the thorax they could be used as reference for the allocation and interpretation of IRT images.

The examined pigs differed in age, weight and chest girth reflecting inhomogeneous pig populations on farms and also pigs of the same age group. As expected, age was not correlated with body diameters, because pigs naturally show variations in their body shapes and proportions. Nevertheless, the extent of the lung was found to be in accordance with the descriptions in anatomical textbooks (e.g. Nickel et al., 1999): The dorsocaudal boundary of the lung was located at rib eleven during expiration, while the recessus costodiaphragmaticus reached the 13th rib. In FTS as well as in the CT images, lungs reached the 13th rib on the left and right side independent of age and size of the pig, because the thorax had been fixed with the lung inflated, mimicking the status of inspiration. The inflated air volume was adjusted to approximately 10 ml/kg body weight, so that it was close to the natural tidal volume of the pigs (Stahl, 1967). Slight inaccuracies due to the use of endotracheal tube and breathing bag should be taken into account discussing the expanded lung sizes.

At the level of all vertebrae bodies, height (V = line x.TV in the CT and IRT images) and width (H) were positively correlated with weight and chest girth. Even in animals differing in age and body proportions V and H were proportional.

The transformation of specific localizations in the cross-sectional CT image into specific ROIs of the longitudinal IRT image was mainly based upon the vertical line 7.TV.

Correlation of difference surface temperatures within specific lung ROIs with tissue layer thickness was of particular interest in this study. At five different localizations difference temperatures were highly correlated with tissue layer thickness. The intermediate layer containing the lung was correlated with difference temperature at R7vL (IL = 21 mm, $\Delta\vartheta$ R7vLr = 2.8°C) on the right side

and R10vL on the left side (IL = 22.2 mm, $\Delta\vartheta$ R10vLl = 2.39°C). This strongly supports the hypothesis that thickness of lung tissue is affecting the surface temperature measured by IRT resulting in a higher temperature difference between these lung ROIs and the maximal abdominal ROI.

Ranges of temperature differences at both localizations can serve as preliminary reference values in this limited number of 20 pigs (Table 1). Because of the homogenous, high health status of pigs, these reference limits should be reliable enough to use them as an allocation base for future studies in diseased animals.

In contrast with the intermediate layer containing the lung, the thickness of the superficial layer was negatively correlated with difference temperatures at localizations 7 dL and 7H on the right side resulting from higher absolute temperatures within the respective ROIs. At localization 10vL on the right side thickness of the deep layer, which mainly consists of liver tissue was also negatively correlated with difference surface temperatures. It is known that temperature of liver tissue is approximately 1–2°C warmer than the body core temperature due to metabolism processes. Skin surface temperature with underlying liver tissue has been found to be higher in comparison to other body surface localizations (Henssge et al., 2004).

Internal body temperatures and absolute surface temperatures on the pig thorax were positively correlated. Anaesthesia by itself as well as low ambient temperatures in the cooling chamber led to a decrease in internal body temperatures.

In addition, it could be clearly shown that the presence of ribs influenced surface temperatures of the thorax. In pigs out of this age group all ribs contained bone marrow supplied with blood and ribs were accompanied by intercostal blood vessels. The effect of heat storage in the costal areas might be stronger than the high thermal conductivity of bone tissue by itself, so that costal skin temperature was higher than intercostal skin temperature. To make sure that measurements in different animals are performed under the same conditions, care must be taken, that costal as well as intercostal areas are included in the respective ROIs. Therefore, it is recommended to increase the diameter of the lung ROIs for future practical application of the technique.

In this study, it became clear that correlations between subcutaneous structures (bone, muscle, connective tissue) and skin surface temperatures existed in healthy pigs. The evaluation of paired CT and the IRT images resulted in preliminary reference values for specific lung ROIs which have to be validated in diseased pigs for its practical use in further studies. In general, an appropriate method for a quick and early detection of local and systemic inflammation would be of high impact for all aspects of swine

medicine and husbandry, e.g. monitoring of epizootic diseases, welfare aspects, and quality assurance within the pork production chain.

Acknowledgements

References

Brauer, C., D. Hoeltig, I. Hennig-Pauka, M. Beyerbach, H. Gasse, M. Hewicker-Trautwein, G.-F. Gerlach, and K.-H. Waldmann, 2011: Computed tomography of the pig lung. An innovative approach to the definition of the pulmonary health status. Tierärztl. Prax. G **39**, 205–214.

Brauer, C., I. Hennig-Pauka, D. Hoeltig, F. F. Buettner, M. Beyerbach, H. Gasse, G.-F. Gerlach, and K.-H. Waldmann, 2012: Experimental *Actinobacillus pleuropneumoniae* challenge in swine: comparison of computed tomographic and radiographic findings during disease. BMC Vet. Res. **8**, 47.

Casal, J., E. Mateu, W. Mejía, and M. Martín, 2007: Factors associated with routine mass antimicrobial usage in fattening pig units in a high-density area. Vet. Res. **38**, 481–492.

Diakides, N. A., and J. D. Bronzino, 2008: Medical Infrared Imaging. Boca Raton: CRC Press.

Hansen, M. S., S. E. Pors, H. E. Jensen, V. Bille-Hansen, M. Bisgaard, E. M. Flachs, and O. L. Nielsen, 2010: An investigation of the pathology and pathogens associated with porcine respiratory disease complex in Denmark. J. Comp. Pathol. **143**, 120–231.

Harder, T. C., and P. Huebert, 2004: Development and application of a nonaplex RT-PCR for simultaneous detection of mycoplasmal and viral agents associated with the porcine respiratory disease complex. Proc. 18th Pig. Vet. Soc. Congress, Hamburg, Vol. **1**, 341.

Hartmann, J., and J. Fischer, 2001: Calibration and investigation of infrared camera systems applying blackbody radiation. Thermosense **23**, 402.

Heinritzi, K., and J. Beisl, 1995: Untersuchungen zur Verwendbarkeit der Sonographie beim Schwein. Dtsch. tierärztl. Wschr. **102**, 4–15.

Hennig-Pauka, I., R. Koch, D. Hoeltig, G.-F. Gerlach, K.-H. Waldmann, F. Blecha, C. Brauer, and H. Gasse, 2012: PR-39, a porcine host defence peptide, is prominent in mucosa and lymphatic tissue of the respiratory tract in healthy pigs and pigs infected with *Actinobacillus pleuropneumoniae*. BMC Res. Notes **5**, 539.

Hensel, A., M. Ganter, S. Kipper, S. Krehon, M. M. Wittenbrink, and K. Petzoldt, 1994: Prevalence of aerobic bacteria in bronchoalveolar lavage fluids from healthy pigs. Am. J. Vet. Res. **55**, 1697–1702.

Henssge, C., B. Madea, M. Benecke, S. Berg, M. A. Geyh, B. Karger, D. Krause, E. Lignitz, and M. A. Rothschild, 2004: Leichenerscheinungen und Todeszeitbestimmung, In: Handbuch gerichtliche Medizin, (B. Brinkmann and B. Madea, eds). Band 1. Berlin: Springer-Verlag, pp. 102.

Hoeltig, D., I. Hennig-Pauka, M. Beyerbach, K. Thies, T. Rehm, G.-F. Gerlach, and K.-H. Waldmann, 2008: Comparison of the diagnostic significance of clinical, radiographic and ultrasonographic results after an experimental aerosol infection with *Actinobacillus pleuropneumoniae* in pigs. Berl. Münch. Tierärztl. Wschr. **121**, 422–431.

Hoeltig, D., I. Hennig-Pauka, K. Thies, T. Rehm, M. Beyerbach, G.-F. Gerlach, K.-H. Waldmann, and FUGATO-consortium IRAS, 2009: A novel Respiratory Health Score (RHS) supports a role of acute lung damage and pig breed in the course of an *Actinobacillus pleuropneumoniae* infection. BMC Vet. Res. **5**, 14.

Infratec GmbH: Benutzerhandbuch VarioCAM high resolution, Stand April 2009.

Klein, C., 1999: Sonographie der Lunge und Analyse der Atmungsmechanik mittels Impuls-Oszilloresistometrie beim lungengesunden und pneumoniekranken Ferkeln und Läuferschwein. Published doctoral thesis, University of Leipzig.

Leiner, G., B. Franz, K. Strutzberg, and G.-F. Gerlach, 1999: A novel enzyme-linked immunosorbent assay using the recombinant *Actinobacillus pleuropneumoniae* ApxII antigen for diagnosis of pleuropneumonia in pig herds. Clin. Diagn. Lab. Immunol. **6**, 630–632.

Myer, C. W., 1979: Radiography review: the alveolar pattern of pulmonary disease. J. Am. Vet. Radiol. Soc. **20**, 10–14.

Nickel, R., A. Schummer, and E. Seiferle, 1999: Lehrbuch der Anatomie der Haustiere, Band II Eingeweide, 8. vollständig neubearbeitete Auflage, Berlin: Parey Buchverlag.

Opriessnig, T., L. G. Giménez-Lirola, and P. G. Halbur, 2011: Polymicrobial respiratory disease in pigs. Anim. Health Res. Rev. **12**, 133–148.

Reinhold, P., B. Rabeling, H. Guenther, and D. Schimmel, 2002: Comparative evaluation of ultrasonography and lung

function testing with the clinical sings and pathology of calves inoculated experimentally with *Pasteurella multocida*. Vet. Rec. **150**, 109–114.

Rieger, M. A., 2005: Beurteilung der Lungengesundheit von Schweinen aus verschiedenen Haltungssystemen mittels BAL und Lungenhistologie, Projekt 030E370.

Schuster, N., and V. G. Kolobrodov, 2004: Infrarotthermografie, 2nd edn. Berlin: Wiley-Vch.

Siewert, C., B. Brosig, S. Döll, D. Rohweder, S. Dänicke, and H. Seifert, 2010a: Differenzverfahren zur Analyse von Temperaturverteilungen im Infrarotbild am Beispiel von induziertem Fieber beim Schwein – Erste Ergebnisse. In: 41. Wissenschaftliche Tagung der Deutschen Gesellschaft für Medizinische Physik (DGMP 2010), (Hrsg.: N. Hodapp, J. Hennig and M. Mix, eds). Freiburg: Tagungs-CD, pp. 510–512.

Siewert, C., D. Hoeltig, C. Brauer, H. Seifert, and I. Hennig-Pauka, 2010b: Medical infrared imaging of the porcine thorax for diagnosis of lung pathologies. Vancouver: Proceedings of the 21th International Pig Veterinary Society Congress, Vol. II, pp. 663.

Silverman, S., and P. F. Suter, 1975: Influence of inspiration and expiration on canine thoracic radiographs. J. Am. Vet. Med. Assoc. **166**, 502–510.

Stahl, W. R., 1967: Scaling of respiratory variables in mammals. J. Appl. Physiol. **22**, 453–460.

Straw, B. E., S. J. Shin, and A. E. Yeager, 1990: Effect of pneumonia on growth rate and feed efficiency of minimal disease pigs exposed to *Actinobacillus pleuropneumonia*e and *Mycoplasma hyopneumoniae*. Prev. Vet. Med. **9**, 287–294.

Verschakelen, J. A., L. Van Fraeyenhoven, G. Laureys, M. Demedts, and A. L. Baert, 1993: Differences in CT density between dependent and nondependent portions of the lung: influence of lung volume. Am. J. Roentgenol. **161**, 713–717.

Wandtke, J. C., R. W. Hyde, P. J. Fahey, M. J. Utell, D. B. Plewes, M. J. Goske, and H. W. Fischer, 1986: Measurement of lung gas volume and regional density by computed tomography in dogs. Invest. Radiol. **21**, 108–117.

Zaproudina, N., V. Varmavuo, O. Airaksinen, and M. Naerhi, 2008: Reproducibility of infrared thermography measurements in healthy individuals. Physiol. Meas. **29**, 515–524.